SRRB FINAL REPORT:

Automatic movement detection and continuous monitoring of events and subsurface conditions at the Rest and Be Thankful

M. W. Khan[1], James Martin[1], S Dunning[2], R Bainbridge[2] and M Lim[1]

[1] Faculty of Engineering and Environment, Northumbria University, Newcastle, NE1 8ST, UK.

[2] Department of Geography, Newcastle University, Newcastle, NE1 7RU, UK.

Table of Contents

EXECUTIVE SUMMARY

The stretch of the A83 road that passes through the Rest and Be Thankful is subject to a chronic and persistent landslide risk. This location is crucial, both as a tourist stop and as a significant pinch point that provides access to the western region of Scotland. It is significantly impacted by a high frequency of landslides, which typically occur in association with heavy rainfall, but as yet direct associations between slope failures and rainfall thresholds have not been consistently reliable. Part of the reason may be associated with the propagation of rain and groundwater through the slope material. Stakeholders have often noted precursory deformation in the area, which sometimes develops into debris flows that threaten road operations. In addressing the challenge of detecting landslides, we have employed both visual and passive seismic continuous monitoring approaches. The visual method involves the use of Particle Image Velocimetry (PIV) applied to near real-time streamed time-lapse photographs, while the new passive seismic monitoring is carried out using ground movement sensors. PIV involves analysing the movement of particles (pixels) from time-lapse photographs to determine the magnitude and direction of slope movements, providing a unique chronology of progressive slope movement. We have worked to make this operational by adding the functionality to automatically alert designated operators when change is detected from the most recent image. However, dedicated operators are required to set locally specific thresholds and areas of interest, to ensure the processing is running, and to validate outputs. The passive seismic approach has been demonstrated to potentially detect and even locate events, but the continuous data streaming that is required limits its operational feasibility with the current infrastructure and signal strength at the site. The best option would be to further develop the system for *in situ* processing and only stream alerts if a set threshold was detected, which would require an in-depth study of the specific signals relative to ambient noise. The passive seismic system also holds exciting and demonstrable potential to detect changes in ground moisture conditions that may be a more direct indicator of critical slope conditions than rainfall, with far lower power and communication links required to achieve the desired data. The use of passive seismic monitoring in combination with co-located electroseismic sensors is introduced as a powerful new combination for the monitoring of the near-surface water saturation.

1. Particle Image Velocimetry

Particle Image Velocimetry (PIV) is an image comparison technique originally developed to detect and measure the movement of particles in a fluid or gas. The principles underlying the image comparison have been extended here to the detection and monitoring of slope movement in a dynamic natural environment. A high-resolution Single Lens Reflex camera was originally located on the hillside opposite the A83 road in a weatherproof cabinet by Newcastle and Northumbria Universities, and subsequently replaced with a permanent installation with secure power. The images obtained by the camera are divided into small regions called the interrogation areas (IA). The corresponding IAs from two images, for example: image A captured at the time t1 and image B captured at t2 are cross-correlated to obtain the displacement at t2 = t1 + Δt along the horizontal (x) and vertical (y) directions of the imaged tracers. Once the displacement has been determined, the x-component u and the y-component v of the velocity vector can be calculated if Δt is known. This concept is illustrated in Figure 2 for one IA.
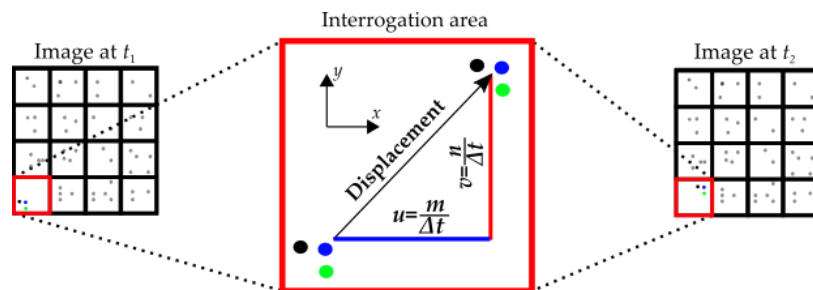
The cross-correlation between two images is implemented as Eq. (1), full derivation is given in Appendix 2.

$$C(m,n) = \sum_i \sum_j A(i,j)\, B(i-m, j-n) \tag{1}$$

The purpose of this research has been:

- To develop a robust automatic change detection software for the new dual camera installation

- To develop a region of interest tool so that specific areas of the slope can be automatically reported on if necessary

- To develop a new grid-based slope system to help unify the dual camera perspectives and improve the clarity of reporting on the new system

- To use the new grid-based reporting system to detect and alert via email a key user group of any movement beyond an agreed threshold

- To train Jacobs engineers to run the software for specific areas and to use this within their regular reporting of slope movements. Comprehensive, step-by-step instructions have also been provided to Jacobs and are included as Appendix in the provided documents.

The camera was aimed primarily at the slope above the A83 road to enable the monitoring of slope movement. Photographs of the slope were taken at typically 15-minute intervals. By comparing two images (photographs) captured at different times, it is possible to detect

changes in the slope, including those that indicate movement. This approach enables the identification of precursory signs of potential slope failure, allowing for timely intervention/inspection to assess the slope area identified. Additionally, ongoing monitoring through image comparison provides valuable insights into the stability of slopes, facilitating the development of effective mitigation strategies to reduce the risks associated with slope movement.

PIVlab is open-source software that was originally developed for airflow monitoring, utilizing high-speed camera sampling rates. Modifications were made to the software to optimize it for landslide monitoring, including adjustments to its algorithms and data processing capabilities. These customizations were necessary to enable PIVlab to accurately and effectively analyse the movement of slope surface structure in the context of landslide monitoring. The software modifications implemented have involved:

Region of Interest

The built-in region of interest (ROI) tool was limited to selecting rectangular ROIs. Consequently, when inspecting the entire slope, both the A83 and the background sky would be included, resulting in vectors generated by clouds and cars on the A83, which were not relevant to slope change detection. To address this issue, a versatile freehand ROI tool was integrated, enabling the selection of multiple ROIs of any shape. This ensured that the software exclusively processed the slope or the specific areas of interest.

Image Duration calculation

PIV requires an accurate calculation of movement vectors based on the elapsed time between two images. The original version of the software was limited to using a predetermined elapsed time value. However, in the modified version, this limitation was addressed by enabling real-time calculation of the period between images using the metadata associated with the image files. As a result, the software now automatically calculates the time duration between the two images it is processing.

Image registration

A robust image registration algorithm was developed to counteract the noise generated by camera vibrations resulting from strong winds. This algorithm ensured that the images captured during high-wind events were properly aligned, mitigating distortions and inaccuracies that could have degraded to efficacy of image comparison. The inclusion of this

algorithm highlights the attention paid to ensuring that the software was optimized for accurate and reliable performance in challenging environmental conditions. Figure 1(a), show the noisy vectors generated by camera movement due to wind vibration. These vectors are not observed after image registration as shown in Figure 1(b).

(a) Before phase alignment   (b) After phase alignment
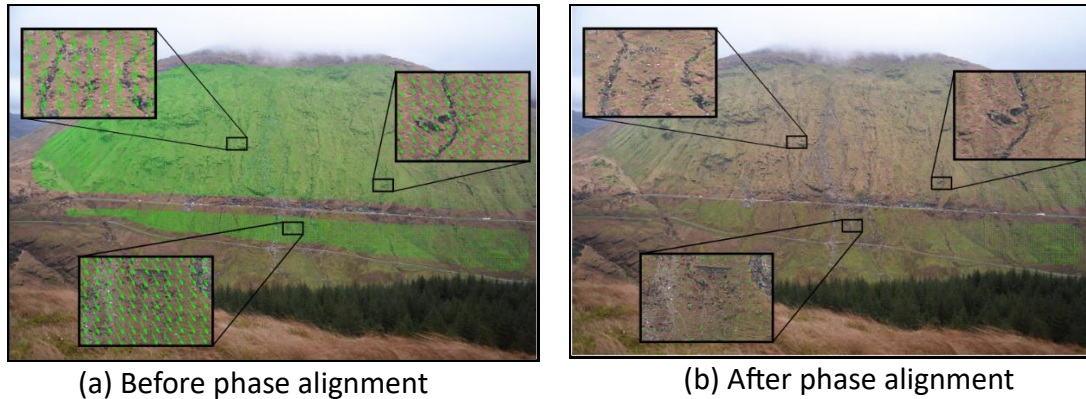
Figure 1. Phase alignment of two images 15 minutes apart [REF1]. Left: Vectors generated shows direction and magnitude of misalignment. Right: After phase alignment vectors magnitude significantly decreased.

Denoising Filters

A filtering mechanism was integrated into the software's output processing to address and eliminate spurious readings caused by factors such as vegetation movement and inadequate/variable lighting conditions on the slope. The purpose of this feature was to enhance the accuracy and reliability of the output generated by the software. By effectively removing this noise, the software became more efficient in its ability to detect and monitor slope movement, thereby improving its overall effectiveness in providing reliable results. The filtering is done by converting the vectors into visual domain, this is followed by applying an erosion filter on the visual representation of the vectors. Erosion filters serve as specialized tools in morphological image processing, designed to selectively eliminate pixels along the periphery of objects within an image. These filters are particularly effective at mitigating visual disturbances, often manifested as diminutive, isolated patches in the visual domain. By eradicating the borders of these small, noisy patches, the filters substantially reduce visual clutter. Additionally, erosion filters are capable of attenuating the boundaries of patches caused by genuine slope movements. While the core of these larger patches may remain, their peripheries are effectively minimized. Consequently, the output generated by erosion filters primarily encapsulates authentic movements, with a significant reduction in extraneous noise.

The erosion filtering process described above reduces noise but is indiscriminate and so has the potential to also remove vectors that are a product of genuine slope movement. Working under the assumption that erosion filtering will remove most of the noisy vectors and only a small portion of slope movement vectors, the results can then be run through a counter process called dilation filtering. As the name suggests dilation expands the mask where filtered (and non-erroneous) slope movement is detected. This procedure effectively restores the full PIV dataset in areas not affected by feature edge effects. The erosion and then dilation filtering of vector outputs successfully eliminates most of the non-slope movement vectors, but occasionally small numbers of noisy vectors remain and could potentially still trigger a false alarm. This is particularly problematic for scenarios where false alarms lead to direct costs such as the closure of an asset like the A83 or mobilization of geotechnical staff to conduct in-person evaluation.

The image generated through erosion-dilation filtering is subsequently overlaid onto the original, non-filtered vectors produced by PIVlab. This processed image serves as a selective mask, isolating regions where authentic slope movement has been detected. As a result, only vectors corresponding to these masked regions are retained, effectively eliminating extraneous data. This, stepwise filtering process is demonstrated in Figure 2, where the input and output of the filters are displayed.
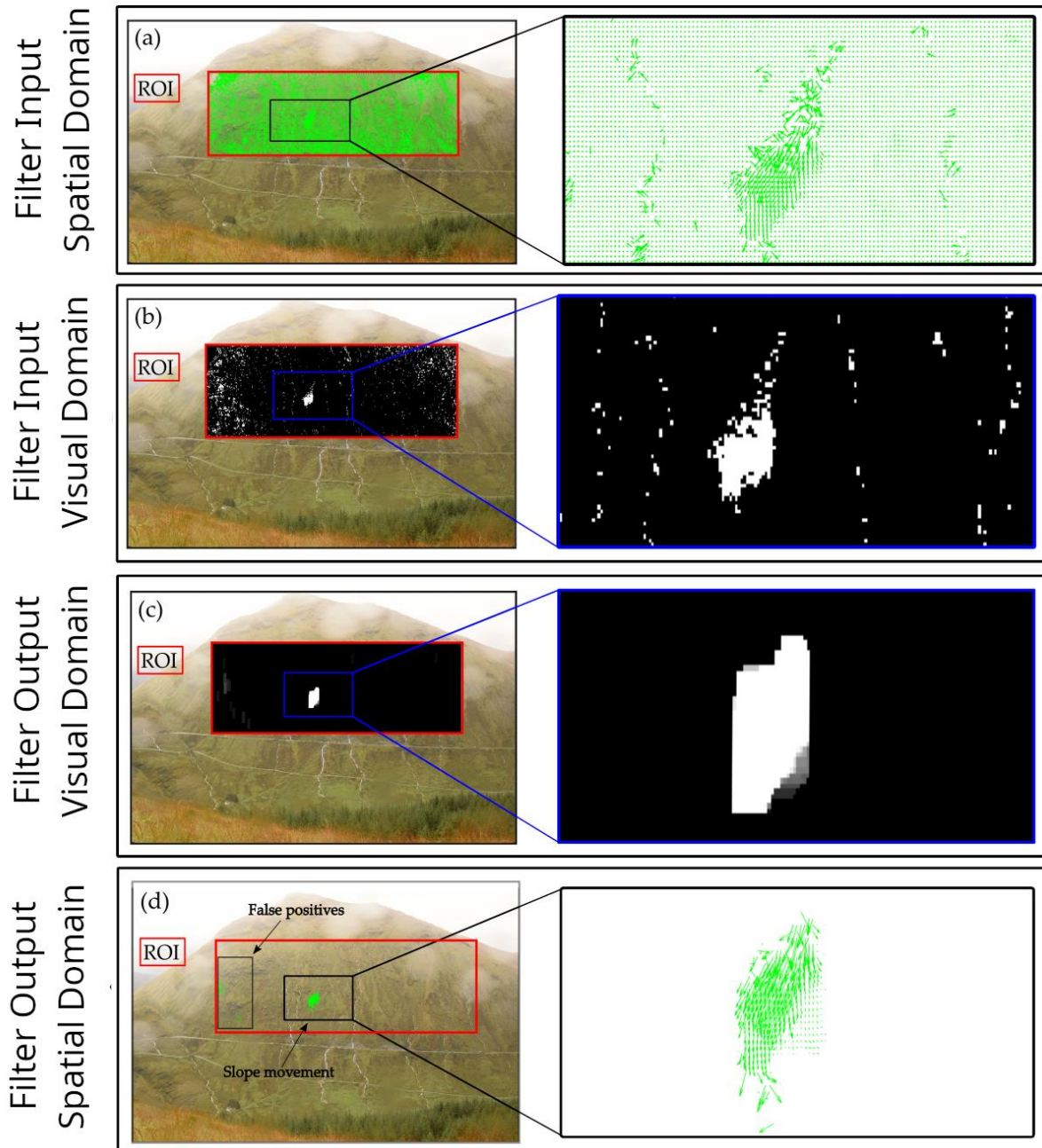
Figure 2. Workflow of morphological filtering for vector frame refinement [REF1].

In September 2018, a 'slope creep' landslide was triggered as a consequence of precipitation induced by Storm Ali, a meteorological event that impacted the United Kingdom and Ireland in the same year. The time lapse imagery (TLI) data, gathered over a span of 20 days leading up to the landslide event, indicated a consistent pattern of creeping motion. This movement was successfully identified through the utilization of PIVlab software. Initial detection of this motion by PIVlab occurred on September 19, 2018, and was subsequently corroborated by a series of TLIs that consistently indicated movement. Figure 3 presents a sequence of TLIs, which were generated by processing pairs of images taken 24 hours apart. Furthermore, TLIs sampled on an hourly basis from September 21, 2018, are displayed to illustrate that the creeping movement was also discernible on more granular timescales. On

October 9, 2018, a debris-flow originating from a higher elevation on the Rest and Be Thankful slope overwhelmed the area where the creeping motion had been previously observed, as depicted in Figure 3, under the section labelled "post-landslide".
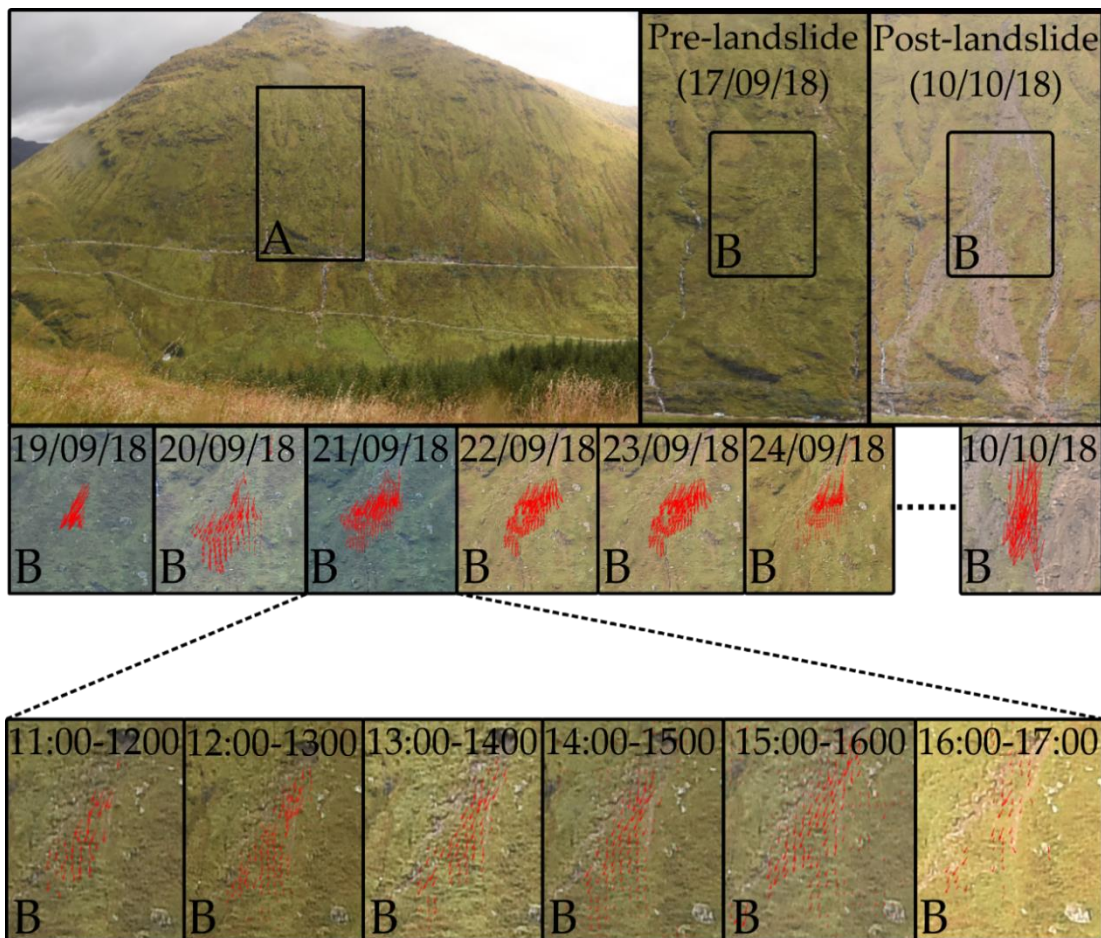
Figure 3. Detection of creep landslide movement. (A) Pre and post failure TLI showing Rest and Be Thankful infrastructure. (B) Series of frames obtained by processing and filtering TLI, capturing slope movement [REF1].

The onset of the slope movement, as identified by Particle Image Velocimetry, demonstrates a correlation with the apex of rainfall, measuring 60mm in the preceding 24-hour period, attributable to Storm Ali on September 19, 2018. This relationship is graphically represented in Figure 4, where daily precipitation levels are juxtaposed with the average velocity of slope movement, as captured by PIVlab, based on 24-hour intervals of TLI data. Subsequent to its initiation, the velocity of the movement exhibits a near-linear escalation, notwithstanding a decline in rainfall. The maximum velocity manifests a temporal lag of approximately 48 hours following the peak rainfall, before attenuating to a null state. Examination of Figure 4 further reveals that the landslide exhibits limited responsiveness to intermittent rain events following the initial event. A marked acceleration in movement is only discernible following a second episode of high-intensity precipitation, during which 80mm of rainfall is recorded on October 9, 2018. On this date, two separate debris-flows emerge from the lower peripheries of the creeping movement zone; however, the primary mass of the creeping movement does not transition into a full-fledged debris-flow.
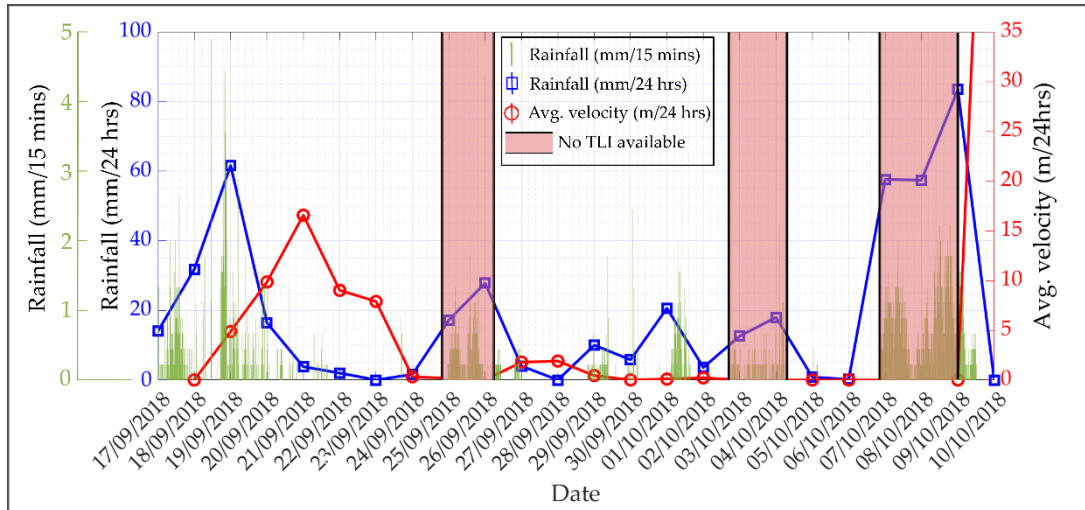
Figure 4. Correlation between slope movement avg. velocity and rainfall observed from 17/09/2018 till 10/10/2018 [REF1].

In November of 2020, in association with an intense precipitation event, another instance of slope creep was observed and documented by PIVlab. The observed movement persisted over an extended period, spanning multiple days. Notably, this particular occurrence did not escalate into a full-scale landslide event. The visualized PIVLab output corresponding to this observed movement is displayed in Figure 5.
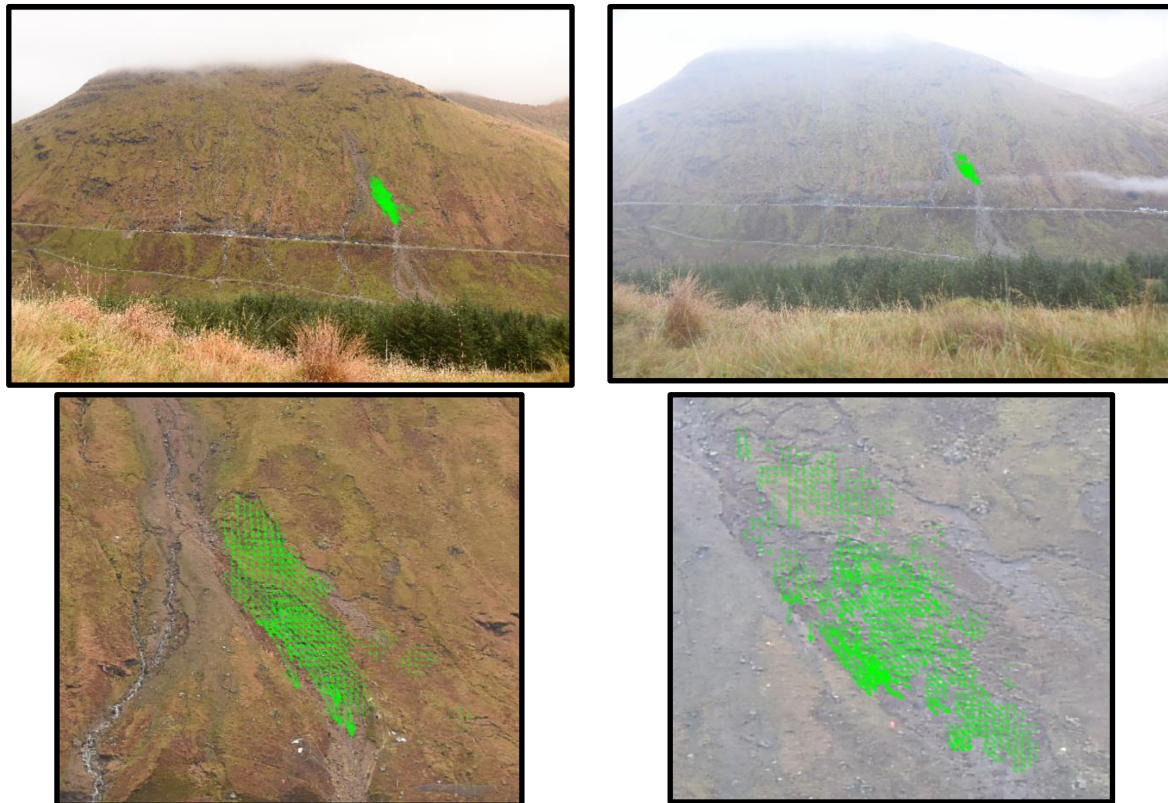
(a) Detection of slope movement between 24-25 Novemeber 2020.

(b) Detection of slope movement between 26-27 Novemeber 2020.

Figure 5. PIVlab output between 24-27 Novemeber, 2020.

Accessing live images

To enable the processing of live captured images, a new feature was implemented that allows users to establish a connection between the software and cloud-based services such as Google Drive. This connection facilitates the automatic downloading of images from the cloud and enables real-time processing. Consequently, the images captured by the camera on-site are uploaded to the cloud software and subsequently downloaded by the software for further processing.

Alert notification

The software has now been enhanced with a real-time alert system that can be run on a networked machine to produce automatic email notifications for stakeholders when movement is detected. By setting a threshold in the software using vector strength (magnitude) and quantity (volume), email notifications can now be generated when the threshold is exceeded. This new feature has been designed providing timely and actionable information to stakeholders and any number of recipients can now be added to the alert list (Figure 6). The inclusion of this alert system demonstrates the commitment to developing a comprehensive landslide monitoring solution that provides both accurate data analysis and effective communication to stakeholders. The final established workflow of PIVlab for slope monitoring is presented in Figure 7.
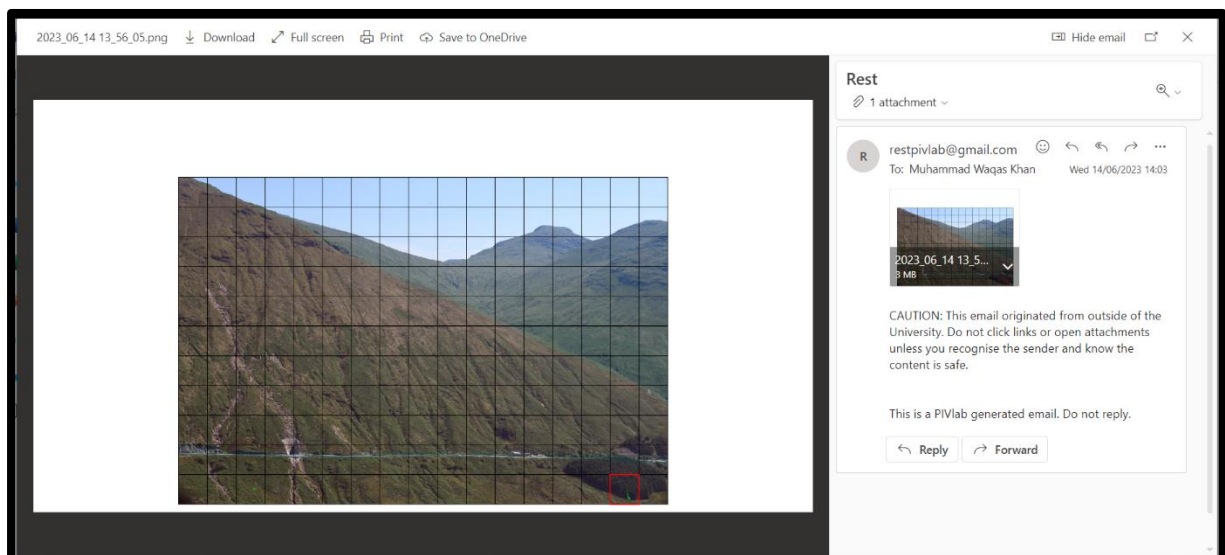
Figure 6. Email alert generated by PIVlab. Emails alerts can be sent to multiple addresses that the user can define in the software.
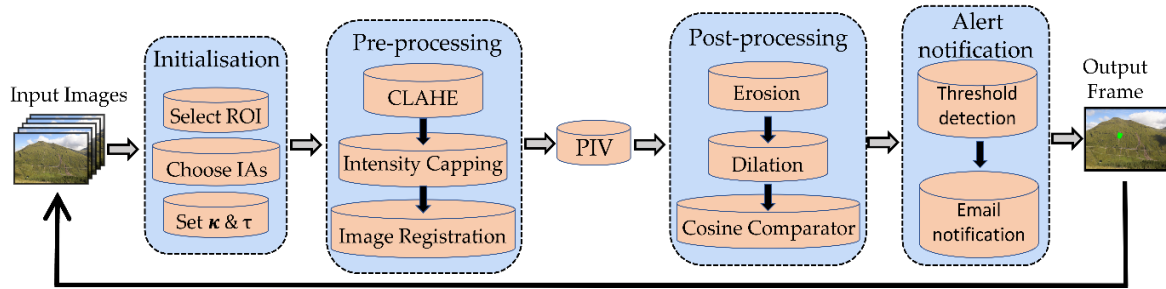
Figure 7. Final workflow of PIVlab algorithm. From image initialization (left) to movement vector generation (right) [REF1].

Limitations

The new software developments implemented have significantly reduced the occurrence of false positives. Nonetheless, it was observed that PIVlab's performance was still affected in poor visibility conditions, particularly when there was cloud/mist/fog between the camera and the slope being monitored. Figure 8, demonstrates some examples where fog, raindrops and poor lighting effect the TLI imagery.

Figure 8. The effectiveness of TLI processing is limited by the occurrence of foggy conditions, raindrops on the camera lens, and low lighting.

This phenomenon caused the software to produce less reliable data, requiring a manual adjustment to the thresholds for monitoring in such conditions. Despite this, the software modifications represent a significant step towards improving landslide monitoring capabilities, particularly when visibility is clear. Further work is required to enhance the software's performance in challenging weather conditions and to expand its potential for use in a wider range of monitoring scenarios. It was observed that the software's monitoring capabilities were limited at night due to the absence of visible light. In response, a near infrared (NIR) camera, capable of analysing slope conditions in low-light and night-time environments was trialled.

Near infra-red time lapse imagery

A near-infrared camera system was implemented to address the inherent challenges of obtaining high-quality imagery in low-light settings. Despite its advantages, this technological solution introduces additional complexities. One such issue is the significant alteration in image attributes like brightness and contrast when conditions transition from low ambient light to complete darkness. Our software currently identifies these fluctuations as noise, thereby complicating subsequent image analysis processes. Figure 9 showcases representative examples of these brightness and contrast variations, while Figure 10 illustrates how the software misconstrues these elements as potential movement. The addition of a NIR camera potentially provides continuous, accurate and reliable data analysis across a range of environmental conditions, but further work is required to balance the use of infrared floodlights, targets and coverage for optimal monitoring during low visibility conditions.

A suggested future direction of research is to co-locate the NIR camera on the opposite valley side with daytime RGB systems to evaluate the ability to capture imagery from a slope-wide perspective. This also opens up the possibility of multiple, mobile, NIR floodlights to illuminate areas of concern on demand.
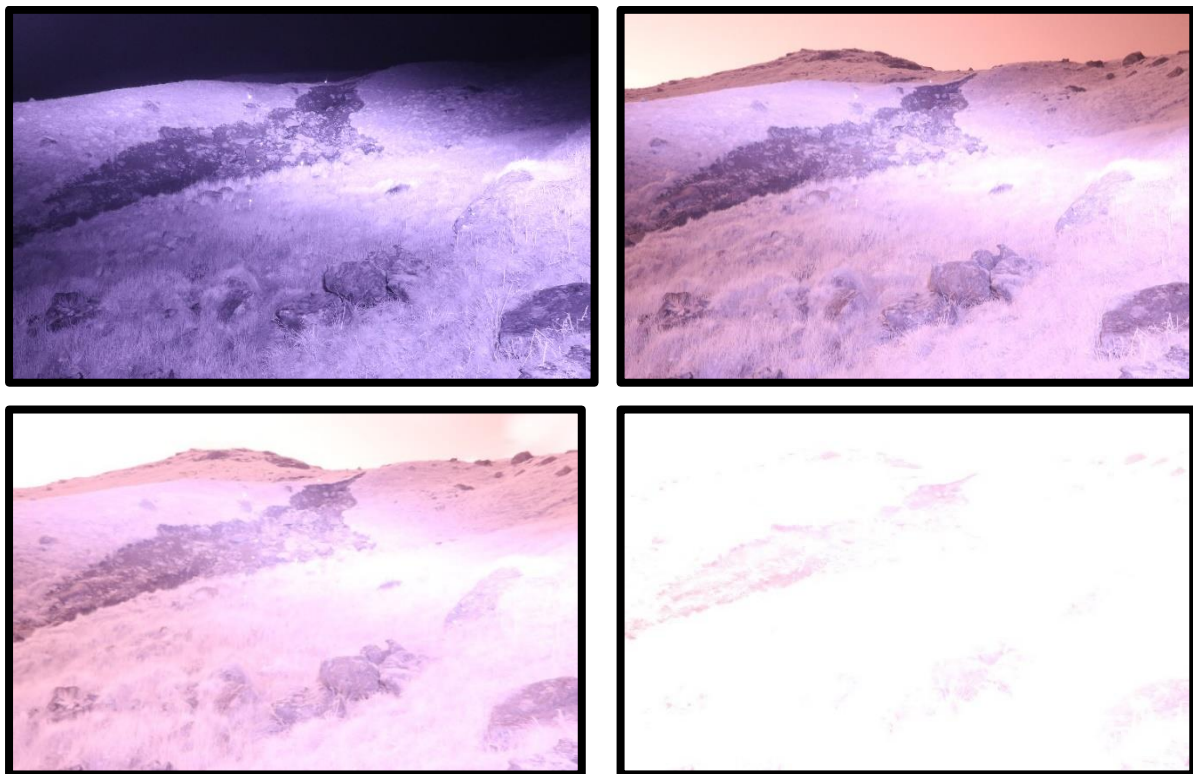
Figure 9. Examples of images captured by NIR camera at night. Pitch dark (upper left) and early dawn (lower right).
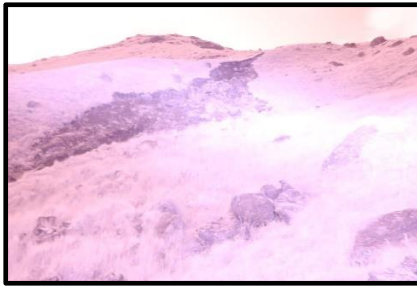
Input Image 1
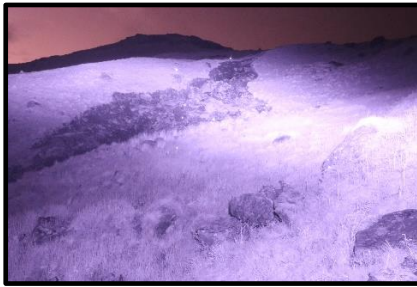
Input image 2
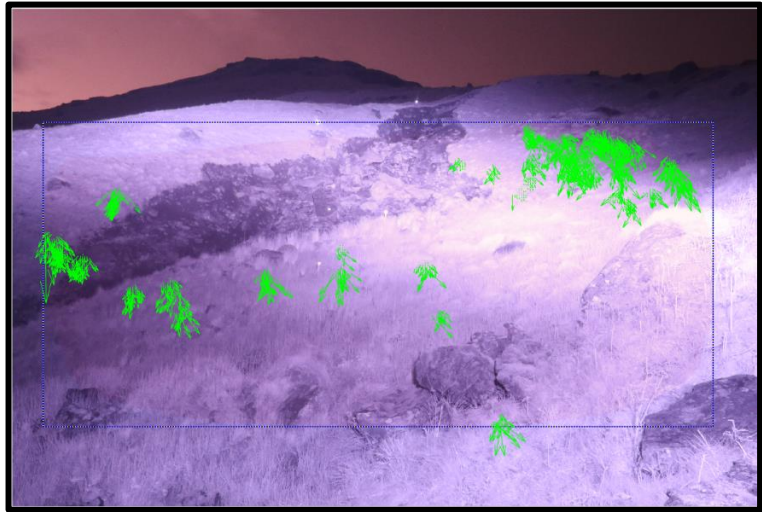
PIVlab output: A large number of false positives are observed when NIR images with different lighting conditions are processed.
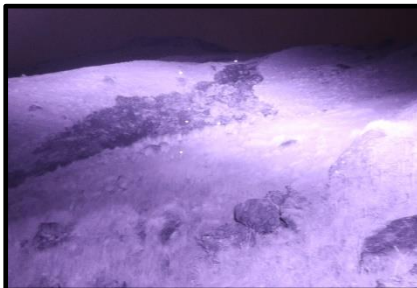
Input Image 3
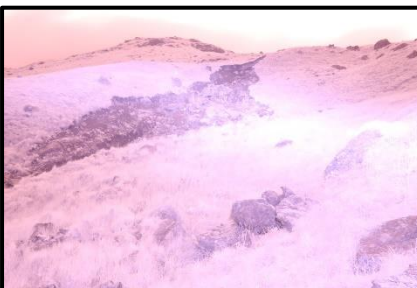
Input Image 4
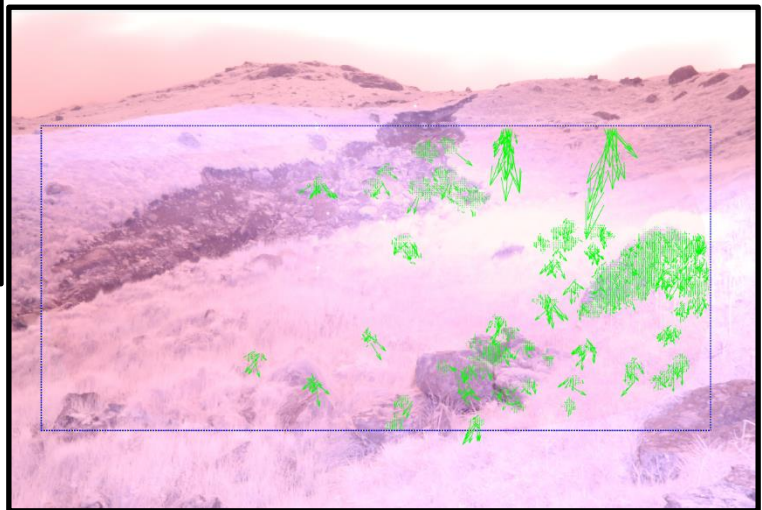
PIVlab output: Coupled with image lighting, the close proximity of the camera to the slope scene can introduce notable discrepancies because vegetation movement becomes more pronounced relative to the changes being detected, thereby potentially inducing errors.

Input Image 5

Input Image 6

PIVlab output: Despite heavy filtering, comparing images with different lighting condition produces significant noise.
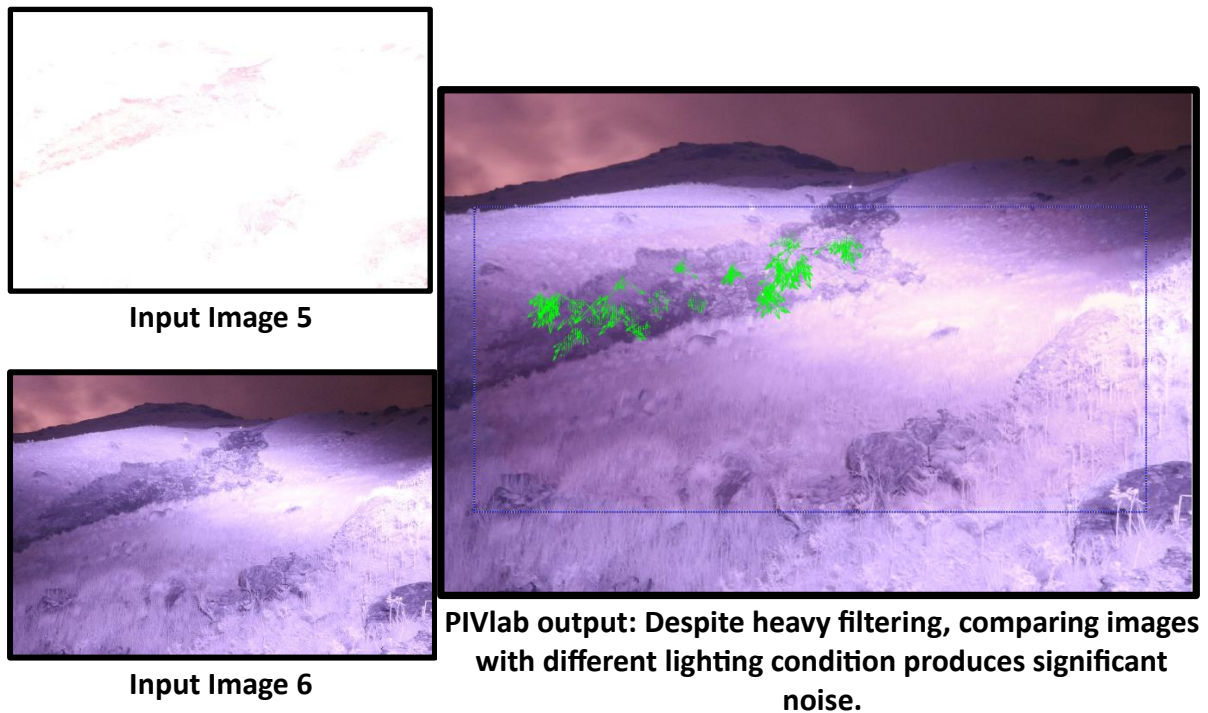
Figure 10. PIVlab output for close-range NIR time lapse imagery.

2. Continuous Monitoring

The seismic monitoring of slope conditions is facilitated by a seismic data logger that has been specifically designed to detect ground vibrations, associated with both slope movement and background noise associated with ground layers and properties. A high fidelity 3-component geophone is used to detect ground motion in each of three mutually orthogonal directions and is not affected by lighting conditions or visibility as with the movement detection approach.

Two versions of the data logger and associated telemetry solutions were developed, one that enables continuous monitoring of the slope for landslide detection and the other that is capable of recording higher fidelity data, but is only activated for discrete periods to enable the monitoring of ground conditions (principally ground saturation).

Event Monitoring Data Logger
The continuous monitoring datalogger samples the geophone analogue signals after high frequencies are eliminated using an analogue anti-alias filter at 400 samples every second on each of its three channels and records it to a multi-media card located in the data logging node. A decimated version of the data sampled at 100 samples per second is streamed to the cloud via Google Services. Despite its capabilities, the potential of the datalogger is currently

constrained by two significant factors: the need for a substantial power source due to its continuous operation and streaming telemetry, and the limited availability of reliable 4G services on the slope, which can hinder the system's performance and deployment location. Nevertheless, with appropriate management of these factors, neither of which is an intractable problem, the datalogger can provide valuable seismic data for continuous slope monitoring and related applications.

Event Monitoring Application

The slope can be monitored to detect landslide events and to track their progression of a landslide event down the slope using the 3-component geophone and continuous monitoring seismic data acquisition node. **Figure 11**, shows 3-component data recorded from the slope above the Rest and Be Thankful road section over a 12 day period from 00:00 hours on the 6th of October 2018. The two horizontal components are oriented in the east (E) and north (N) directions, orthogonal to the vertical component (Z). The seismicity measured on the slope can be used to detect landslide events and to track their progress down the slope, providing a real-time warning of landslide activity. The geophone seismic system provides continuous slope monitoring capability.
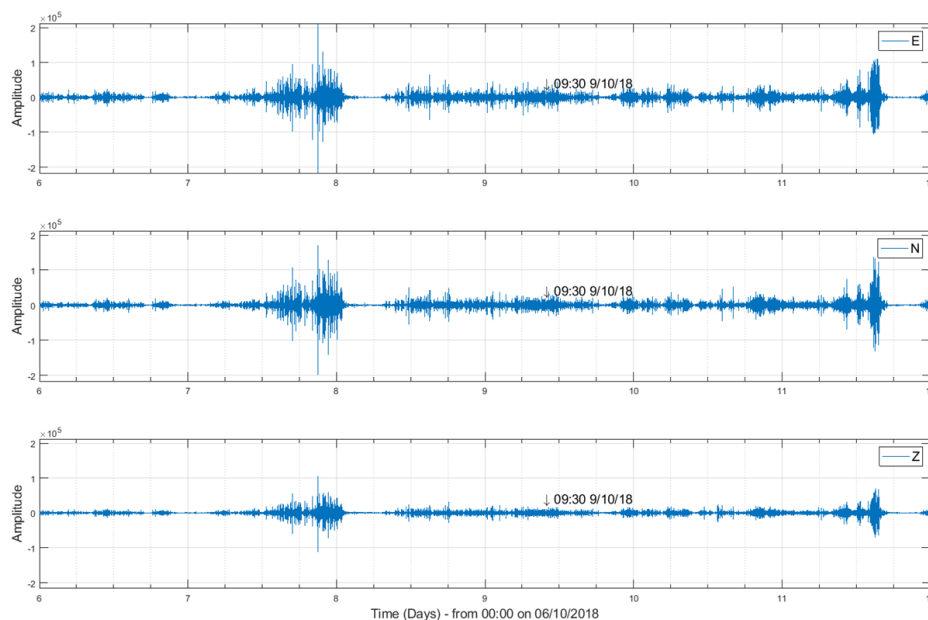
Figure 11. 3-component geophone data recorded from the slope above the Rest and Be Thankful.

Detection and tracking of landslide events is best achieved by monitoring the two horizontal geophone signals. Figure 12 shows example seismic data from a real and verified landslide activity recorded by the N and E horizontal geophone components on the 9th of October 2018, between 14:42:43 and 14:57:43 hours [the events seen on figure 3 at later times are also landslide events, but the hodogram analysis has only been conducted on the primary initial event in this report]. The amplitude of the seismic events can be used to define a threshold to signify the detection of a landslide event and trigger a warning to the A83 road operators.
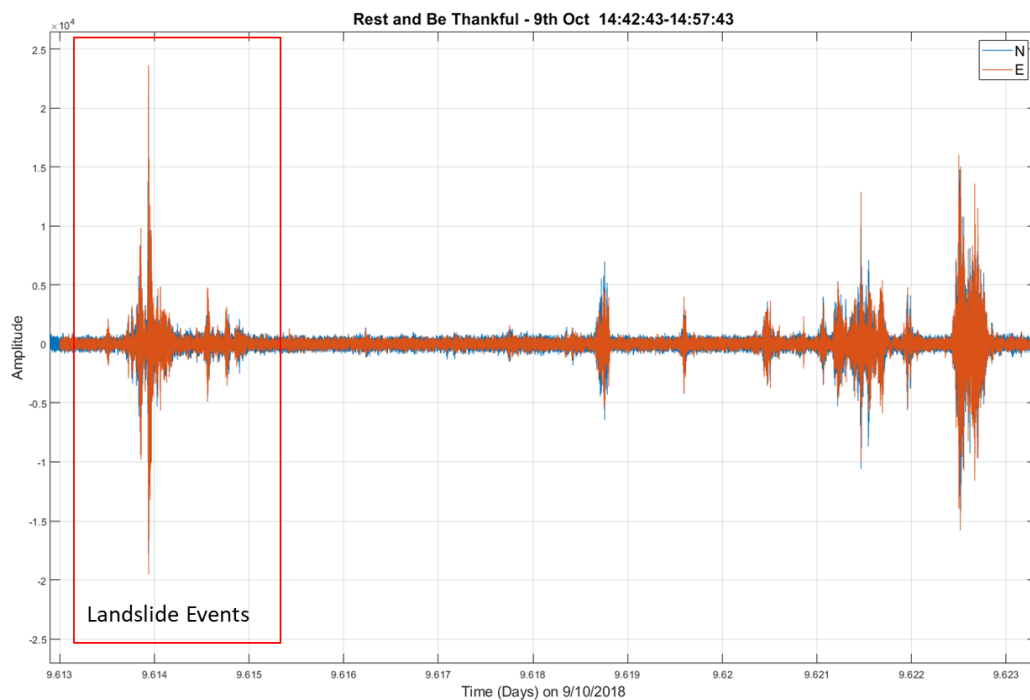
Figure 12. N and E component geophone signals from a verified series of landslide events recorded on the 9th of October 2018.

The three minute period from 14:42:43 is further analysed in Figure 13 through the use of hodograms.

Rest and Be Thankful - 9th Oct from 14:42:43 10s Hodograms
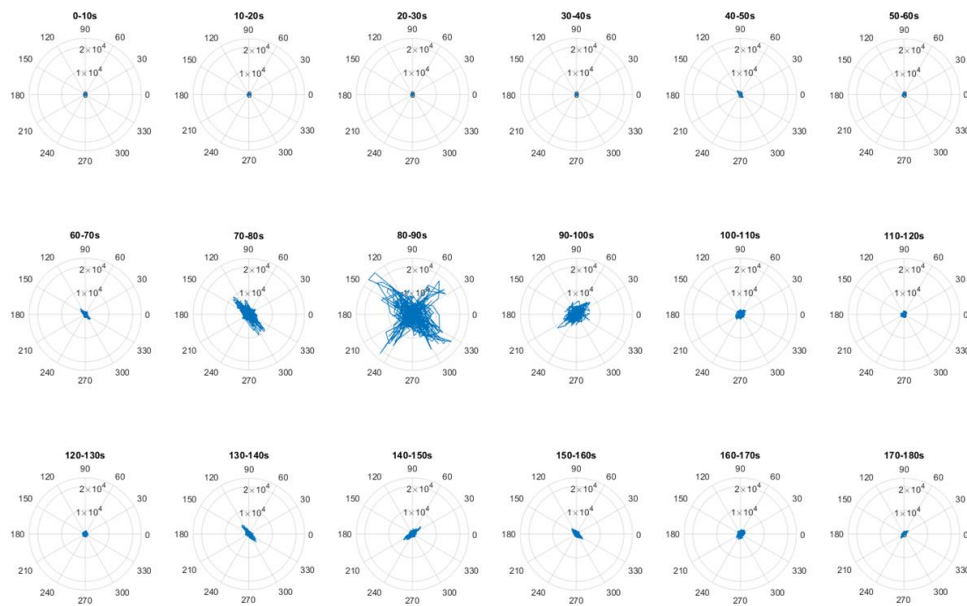
Figure 13. Hodograms constructed from the N and E geophone data from 10s contiguous windows for the 3 minute period from 14:42:43 hours (the data shown within the red box on figure 6).

The amplitudes of the E and N geophone signals for a common time sample can be treated as ordinates, to form a 2 dimensional co-ordinate system. If the E ordinate is plotted in the X direction of a graph and the N ordinate is plotted in the Y direction of a chart, the plotting of E and N co-ordinates for successive time samples traces a hodogram figure. Seismic signals are often rectilinear (they form almost straight line shapes within a hodogram) and their resulting hodograms trace linear figures that point in the direction of the source of the signal. The hodograms in Figure 13 are each formed from 10s of data. The major seismic events within the red box from Figure 12 are seen to exhibit rectilinear behaviour and they point in the direction from which the seismic signal originates relative to the sensor. Note that those directions are sometimes different for adjacent hodograms; indicating different parts of the slope are sliding at different times (e.g. row 2, columns 2, 3 and 4). The hodogram sequence in row 2, columns 2, 3 and 4 indicate two landslide events that occurred within the 30s monitoring period. Firstly, we have the landslide with events aligned NW-SE on row 2, columns 2 and 3 and then a later landslide aligned NE-SW in row 2, columns 3 and 4. The amplitude of the rectilinear events on the hodogram from row 2, column 3 are high because the landslide events are closest to the geophone position within that time period. The two

events are superimposed on one another in hodogram row 2, column 3, as they are both active within the 10s period monitored by that hodogram. Use of at least two geophones at different locations on the slope can accurately track the progression of a landslide through triangulation of their hodograms from common events.

Ground Condition Monitoring Node Design

To circumvent the challenges posed by limited 4G connectivity and power requirements, a different version of the datalogger was developed with enhanced capabilities. This new system has an external Real Time Clock for timekeeping control and is designed to sample data at twice the data rate of its predecessor, collecting half an hour of records every 6 hours and uploading the data files to the cloud. This is followed by enabling the sleep mode to conserve power. To further optimize power usage, a relay-based system was designed to only activate the WiFi router when new data are available for upload. This updated datalogger design enables the telemetry of true 800 samples on each channel as were recorded by the node. The schematic, printed circuit board drawing and actual node are given in Figure 14 and Figure 15.
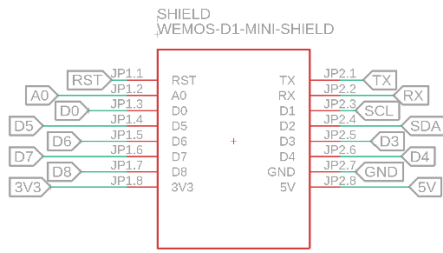
MMC unit (Wemos MMC Shield)
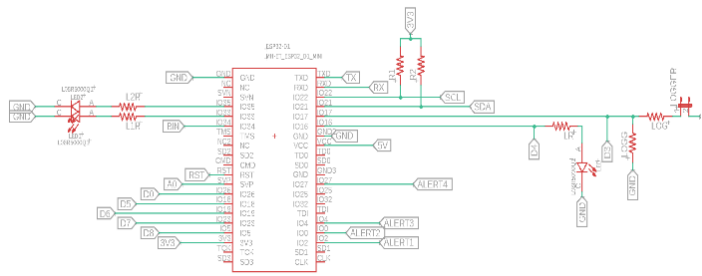
Microcontroller unit (ESP32 WEMOS D1 Mini)
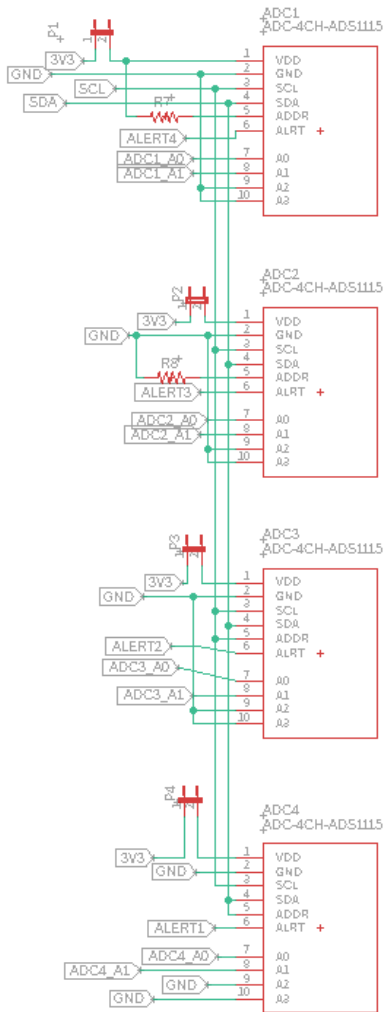
Analogue to digital converter unit

(ADS1115)
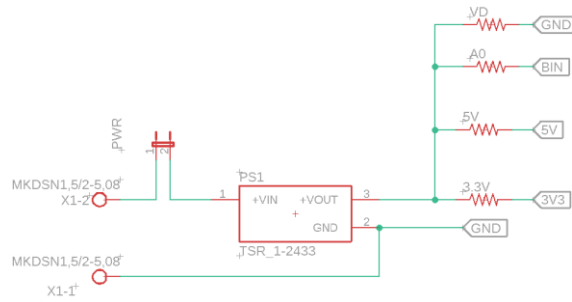
Power supply unit (Traco TSR-2433)
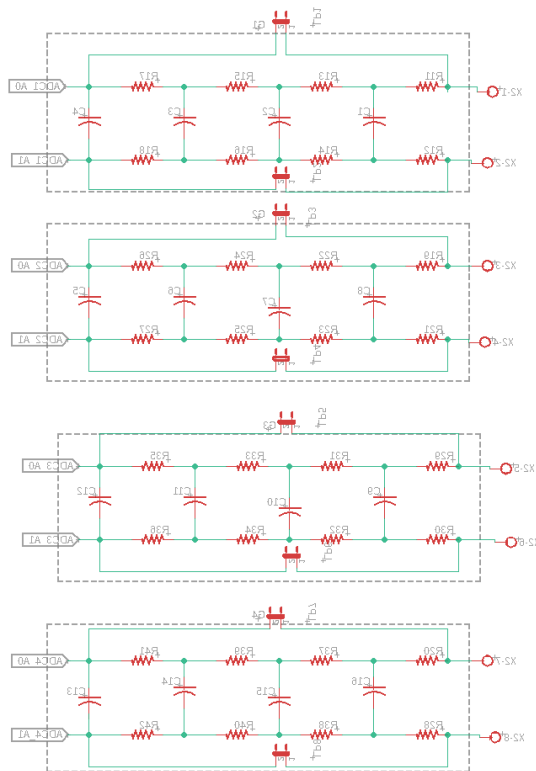
Low pass filter unit (Cutoff 267Hz)

Figure 14. Schematics of Seismic Monitoring Node.
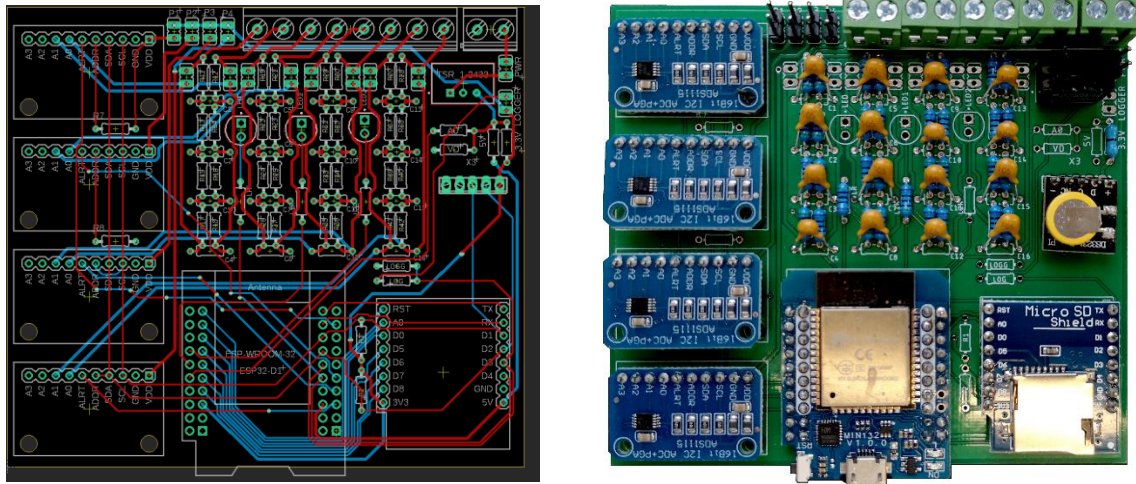
Figure 15. Seismic node drawing (left) and printed circuit board photograph (right).

Ground Condition Monitoring Application

The discrete period monitoring data logger can be configured to be live for planned discrete periods and to be in sleep mode at other times. Such an operational configuration cannot be used to continuously monitor for landslide events but is ideal for near surface condition monitoring where changes are slower and more progressive. Ground condition monitoring has strong potential as a key indicator of failure potential on the slope and is potentially a key missing dataset in monitoring presently conducted at the site. The primary technique for ground condition monitoring is horizontal-to-vertical spectral ratio analysis (HVSR). The HVSR measures the dynamic characteristics of the subsurface using microtremor measurements propagating through the near-surface ground layers. Microtremors are small, barely noticeable seismic waves constantly passing through the earth's surface, the sources of which are ambient. HVSR analysis calculates the ratio of the amplitude of the horizontal and vertical components of these seismic waves in the frequency domain. The resonance frequencies and amplification factors of these tremors can be calculated to assess the response of the soil strata. The resulting $HVSR(f)$ spectrum is plotted as a function of frequency where the peak frequency f_0 corresponds to the fundamental resonance frequency of the site and the amplitude of the curve at f_0 corresponds to the amplification factor. The use of HVSR for slope stability centres on the resonant response of the unconsolidated soil layer being sensitive to its water saturation. The unconsolidated layer thickness above the bedrock on the slope will be constant. The shear-wave velocity in this unconsolidated layer is dependent on the water saturation of the layer, which in turn affects the resonant frequency of the HVSR spectrum.

We can monitor the HVSR resonant peak and use the information as a proxy for water saturation. The water saturation of the unconsolidated layer can rise to the point whereby the soil loses its shear strength and the slope will then be prone to sliding.

The use of electroseismic sensors for near surface condition monitoring has been the subject of recent research at Northumbria University. Electroseismic measurements involve deploying an electrode pair into the near surface to be monitored. The electro-potential between electrodes is measured and recorded at a high data sampling rate using the data logger. The incident passive seismic signals measured and analysed using the HVSR approach described above also generate time varying, dynamic electro-potential signals in the near-surface caused by movement of the water within the soil matrix. These dynamic electro-potential signals are detected by the electroseismic sensors. The amplitude and the spectral bandwidth of the electroseismic signals is sensitive to the water saturation of the near-surface soils; the higher the soil water saturation, the higher the signal amplitude and broader the spectral bandwidth of the electroseismic signal.

A field test has been used to illustrate the use of HVSR and electroseismic monitoring of soil water saturation under controlled conditions. The 3-component seismic sensor and the electrode pair were deployed in a garden lawn. The near-surface layering consisted of a 0.25m thick layer of loam on top of a sandy clay. The lawn was saturated with water using a sprinkler system that that operated for 1.5 hours. Drainage from the loam layer through the sandy/clay subsurface would be slow.

Figure 16 shows the HVSR spectra that were recorded using the 3-component geophone after the sprinkler system was turned off. The colour sequence starts at red and progresses through to yellow following a spectrum sequence. A 30 minute time increment is used between each trace. 9 traces are displayed, conforming to a 4 hour monitoring period. The Log_{10} of frequency is shown on the x-axis, while the amplitude of the HVSR spectra is shown in the y-axis. The 0.25m loam layer has a natural resonant frequency of around 12Hz. The 0.25m thick loam layer is very thin, yet a clear reduction in the resonant frequency peak can be seen as the loam layer naturally drains of water within its matrix. Another striking result is that the peak amplitude of the resonance reduces significantly in amplitude as the loam layer drains.
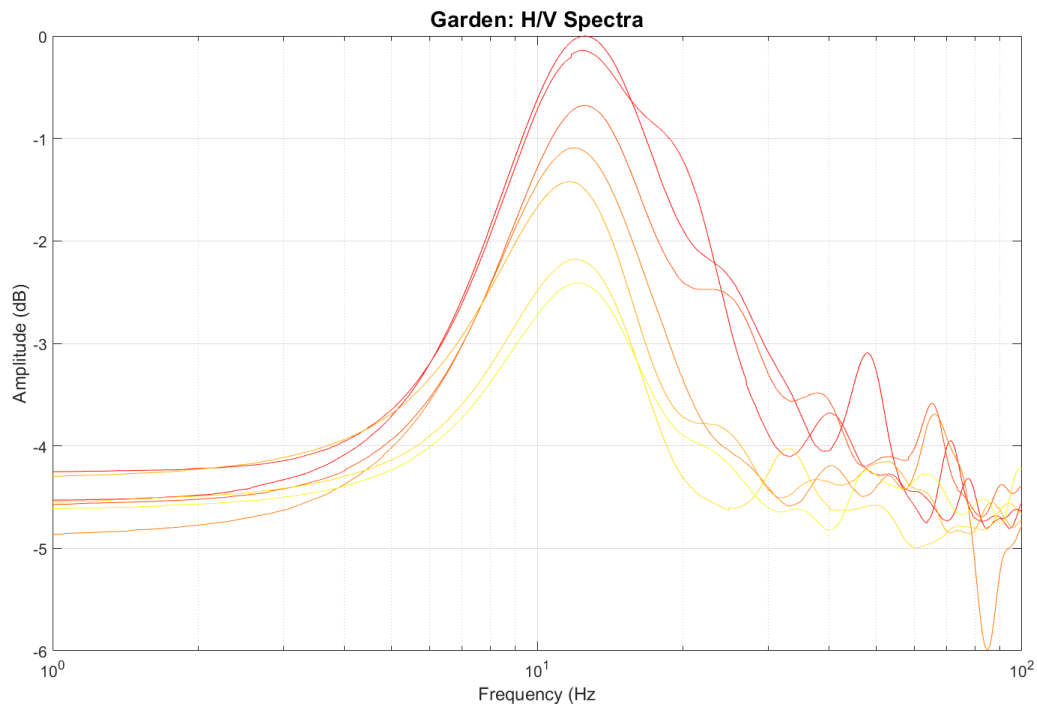
Figure 16. HVSR spectra showing progressive reduction (red through to yellow at 30 minute intervals) of signal amplitudes with the drainage of a 0.25m thick loam layer.

Simple metrics such as the root-mean-square (RMS) amplitude of recorded data traces can be used to monitor for soil saturation. The geophone was planted on the surface of the lawn during the experiment which meant that water droplets falling onto the upper surface of the geophone would generate broadband signals during the wetting process.

Figure 17 shows the RMS amplitude data from vertical geophone seismic and electroseismic recordings. Data are displayed that span the closing phase of the water saturation process and into the loam drainage stage. The data from the vertical geophone component show that the lawn sprinkler was operational up to approximately 18:35. The electroseismic data show that the electro-potential RMS amplitude continues to rise slowly up to 18:35, when the loam reaches its peak water saturation level. The electroseismic RMS data then monotonically reduce in amplitude as the 0.25m thick loam layer slowly drains between 18:35 and 20:45.
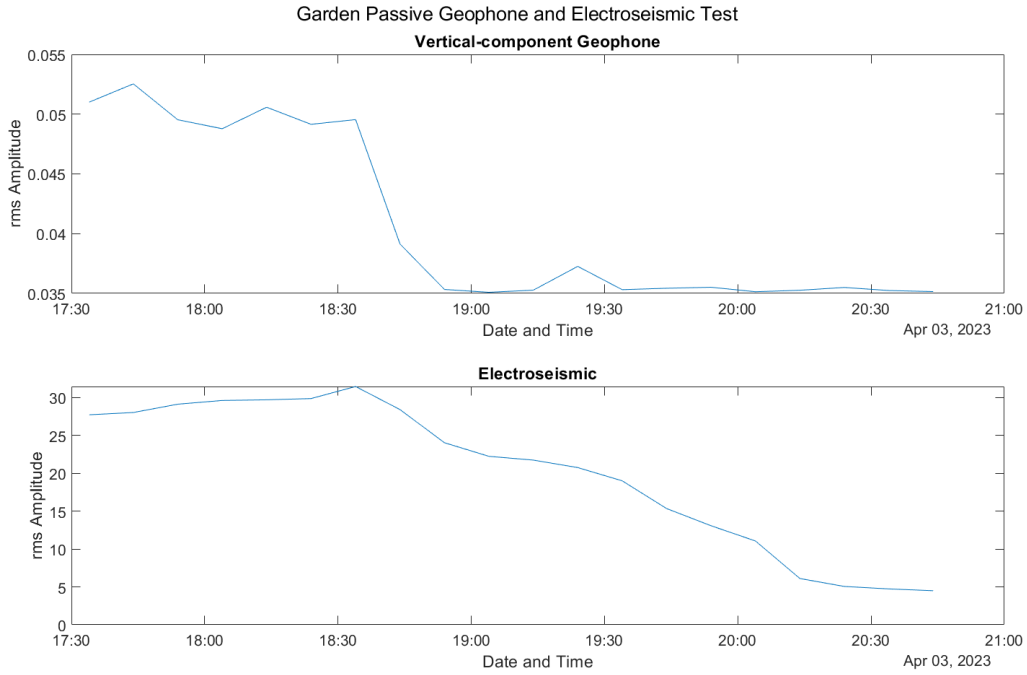
Figure 17. RMS amplitude data from a vertical geophone component (reflecting deeper processes) and electroseismic sensors (reflecting very near surface processes) following the transition from saturation to initial drainage.
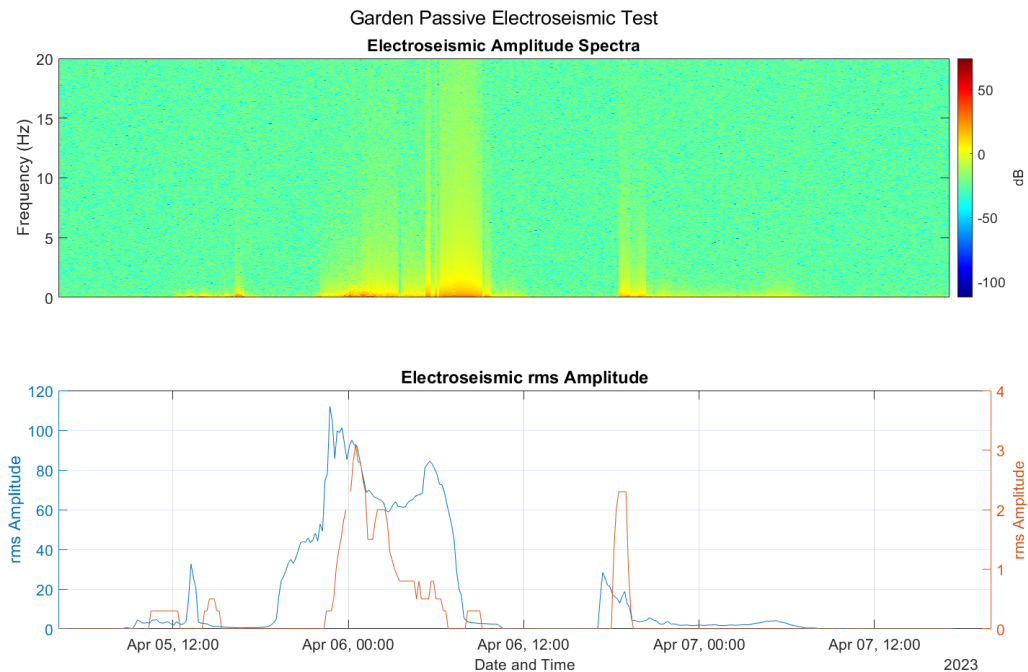
Figure 18. Electroseismic RMS and spectra data directly responding to recorded rain events from a local weather station (2 miles away).

Figure 18 shows an analysis of electroseismic RMS amplitude and spectra data recorded over 3 days when rainfall events were monitored that would increase the water saturation within the 0.25m thick loam layer. Rainfall rate data in mm/hour were obtained from the Cullercoats weather station that is approximately 2 miles from site of the HVSR and electroseismic experiment. The rainfall rate data can, therefore, only reflect an approximation of the actual rainfall at the test site as showers tend to quite localised in both the start and end times and their rainfall rates. The match between the rainfall event time and the RMS amplitude data from the electroseismic sensors, however, is compellingly close. The minor rainfall events lead to a modest increase in electroseismic amplitude. The prolonged rainfall event between 18:00 on April the 5th and 06:00 on April the 6th results in a much higher electroseismic RMS amplitude, as the higher water saturation of the loam leads to high amplitude electroseismic signals being generated. The electroseismic amplitude spectra show that the bandwidth of the electroseismic signals also increases for higher loam saturation levels.

The use of HSVR in combination with co-located electroseismic sensors provide a powerful combination for the monitoring of the near-surface water saturation. The HVSR approach measures changes in soil density while the electroseismic approach measures changes in soil conductivity as soil water saturation changes. Both measurements can be calibrated to allow prediction of when soil water saturation approaches dangerous levels that would cause the soil's shear strength to reduce, increasing the risk of a landslide.

3. Further Work

The use of the HSVR method as a proxy for water saturation estimation in unconsolidated soils is the subject of active research work at Northumbria University. We are also researching a complimentary measurement that involves recording the passive electroseismic signals using an electrode pair. The data loggers developed at Northumbria University are low cost and have four data channels available and so can be used to measure the signals from the 3-component geophone as well as the signal from one electroseismic detector.

The use of 3-component data and electroseismic data for near-surface condition monitoring will be explored further using the geophysical node systems that are planned to be installed on the slope at Rest and Be Thankful should additional funds and planned mitigation works allow.

Recommendations

1. Time-lapse camera analysis developed by the team has already proven to be a valuable and impactful tool, identifying previously undetected areas of movement that have later led to potentially damaging events where severe impacts have been mitigated. Making sure the timelapse system is effectively utilised and operated is key to its success and further setting of appropriate alert thresholds relative to the conditions will help refine the data achieved.

2. NIR imagery has been effectively tested with useable images achieved from slope side camera position and IR flood lights for key areas. Additional testing is required to see the resolution of change detectable in NIR images and the effectiveness of wider scale monitoring from the opposite slope with the NIR camera co-located with the daytime (visible) cameras. NIR floodlights are effective but can cause high contrast issues further and testing is needed to ascertain their optimum set up (sited on-slope or on the opposite side to illuminate specific areas of concern or the whole slope respectively).

3. NIR image consistency requires further work to optimise the image settings and processing. Additional testing will improve the fidelity of NIR surveying by being able to dynamically compensate for dynamic changes in incident near infra-red light on the slope being monitored. Time-lapse image comparison to detect movement on the monitored slope will then be enhanced.

4. If event detection is critical, passive seismic systems have clear potential, but reliable power and streaming signal needs to be improved at the site and dedicated time provided for a detailed study of the various noise sources and frequencies to reduce the detection of false positives.

5. A wider network of seismic monitoring should be considered for better event identification and location, but a more cost-effective solution may be to monitor the impacts against the catch nets on site for more reliable filtering of the most significant events.

6. The passive seismic ground condition monitoring is an exciting new technique that the logging systems now make effective as a potentially operational tool to support and refine the rainfall threshold alerts and improve understanding of how the ground responses are developing during high intensity events.

7. Passive electroseismic monitoring requires more testing but effectively provided a very low cost and low power monitoring system of the ground conditions that could cost-effectively be used at useful scales across the site. This remains cutting edge research however and would need further testing before operationally ready.

Acknowledgements

Appendix 1 – Image Registration via Phase correlation

The idea behind image registration using phase correlation is to capture the linear phase component of a moving image in the frequency domain and which arises as a result of translation in x and y directions of the same image in a spatial domain.

Method: Consider, image $\mathbf{A}(i,j)$ and its shifted version $\overline{\mathbf{A}} = \mathbf{A}(i-m,j-n)$. Taking the fast-Fourier transform of $\mathbf{A}$ and $\overline{\mathbf{A}}$ one can obtain:

$$\mathbf{A}(i,j) \xrightarrow{FFT} \mathbf{X_A}(\omega_1,\omega_2) \tag{A1}$$

$$\overline{\mathbf{A}}(i-m,j-n) \xrightarrow{FFT} \mathbf{X_A}(\omega_1,\omega_2)e^{-j(m\omega_1+n\omega_2)} \tag{A2}$$

where $\mathbf{X_A}$ is the FFT of the fixed image $\mathbf{A}$, m and n are the shifts in $\overline{\mathbf{A}}$ when referenced with $\mathbf{A}$. The next step involves taking the cross-correlation of the Fourier transform of the two images i.e., Equ. (A1) and (A2), which result in

$$
\begin{aligned}
\boldsymbol{T}(\omega_1,\omega_2) &= \frac{\mathbf{X_A}(\omega_1,\omega_2)\overline{\mathbf{X_A}(\omega_1,\omega_2)e^{-j(m\omega_1+n\omega_2)}}}{\left|\mathbf{X_A}(\omega_1,\omega_2)\overline{\mathbf{X_A}(\omega_1,\omega_2)}\right|} \\
&= \frac{|\mathbf{X_A}(\omega_1,\omega_2)|^2 e^{j(m\omega_1+n\omega_2)}}{|\mathbf{X_A}(\omega_1,\omega_2)|^2} \\
&= e^{j(m\omega_1+n\omega_2)} \tag{A3}
\end{aligned}
$$

where $\overline{(.)}$ represents the complex conjugate of a function $(.)$. One can capture the translation in *x* and *y* direction of the moving image by taking the inverse discrete Fourier transform of Equ. (A3).

Appendix 2 – Use of PIVlab

1. On the main screen, press Load Images
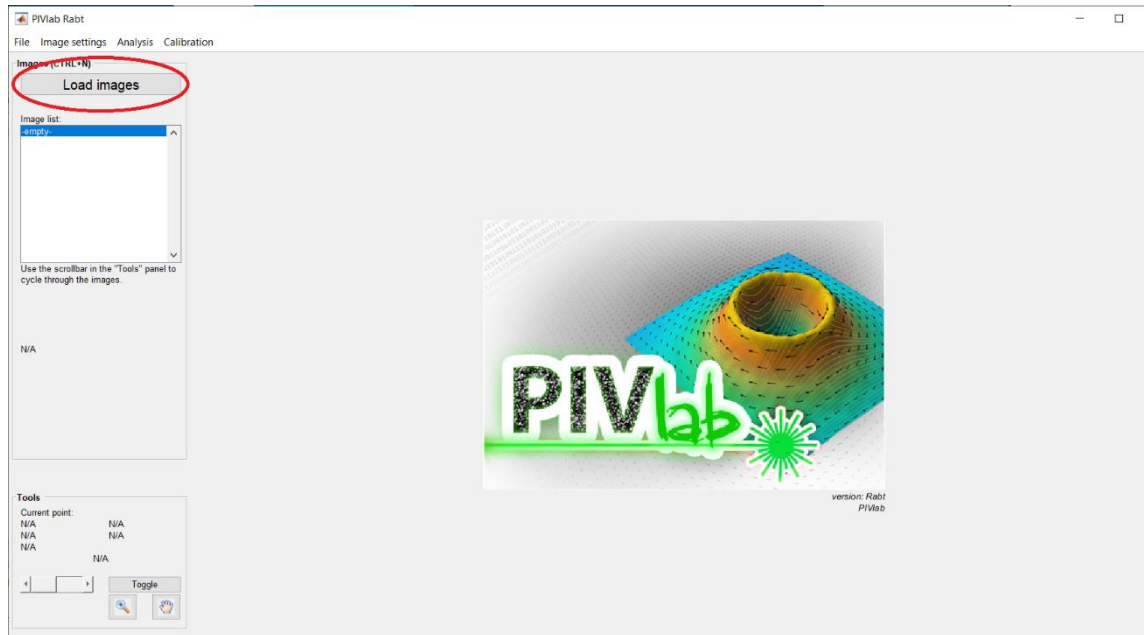
2. Tick process new images, to process new images from google drive. Keep unchecked if this feature is not required.
   Make sure sequencing style selected is 1-2,2-3,3-4.
3. Click select directory button (button with three dots …).
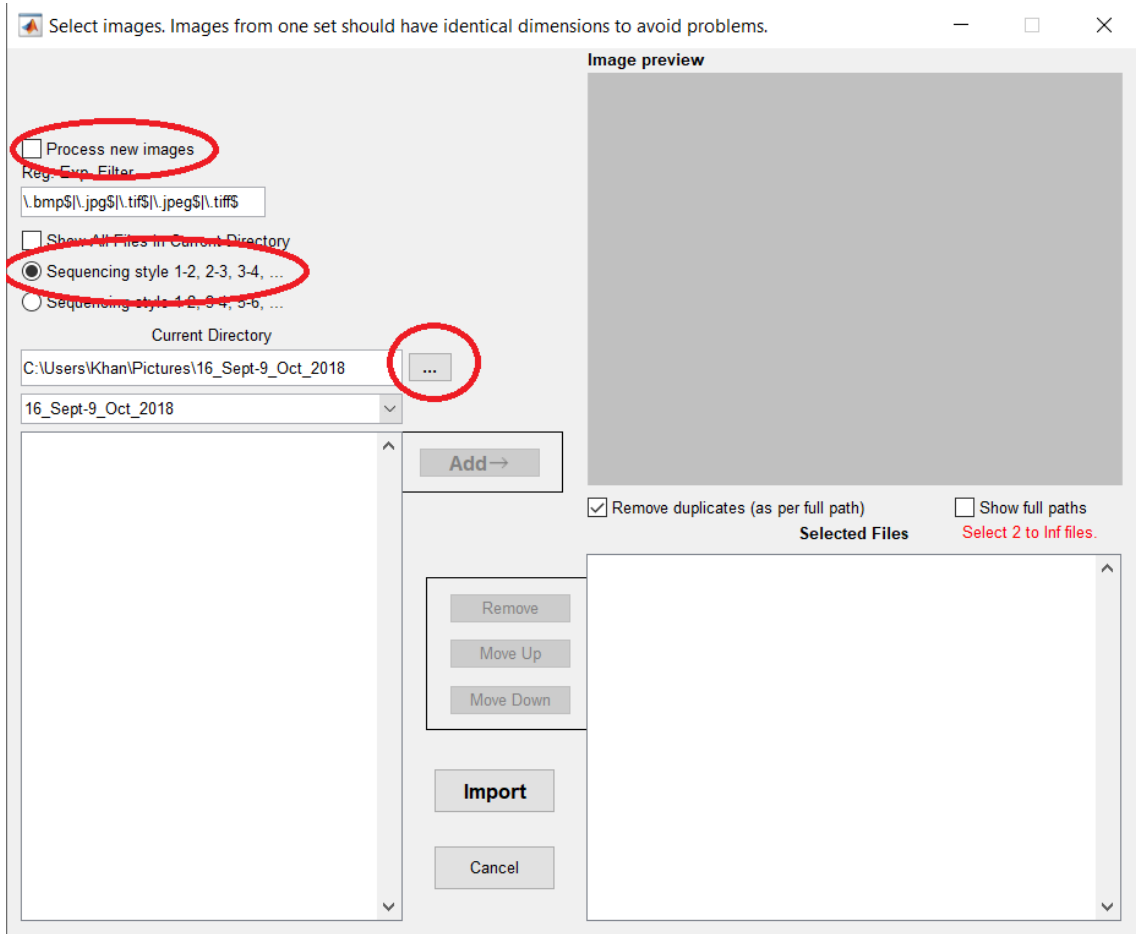
3. Navigate to directory with images and click select folder.
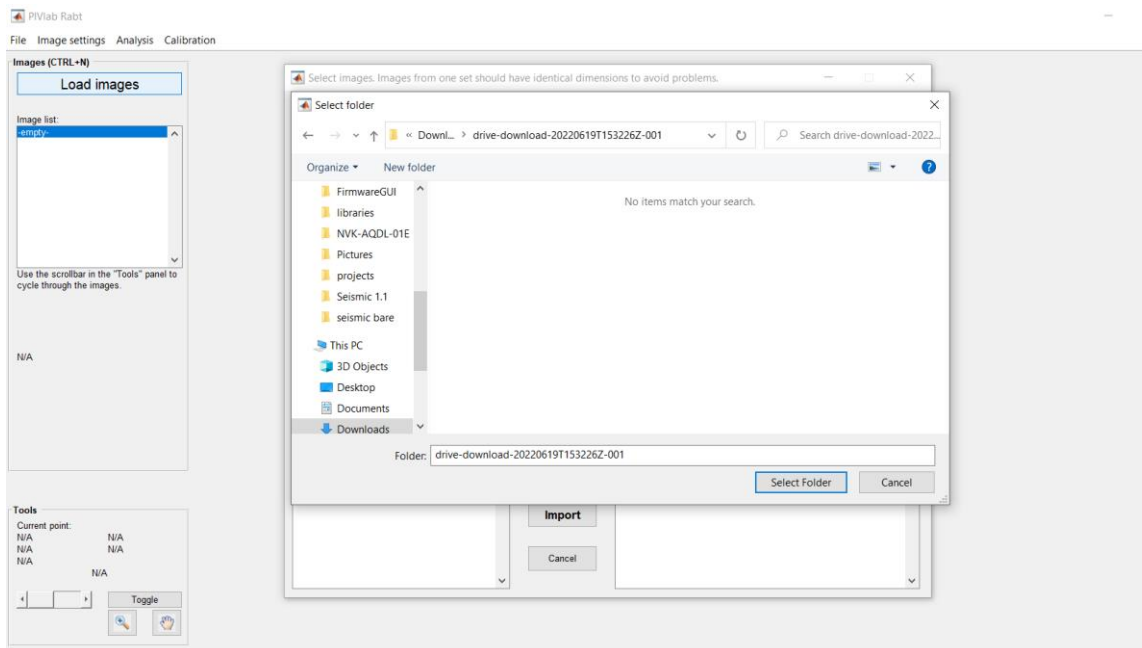
4. Images names will show up on the right tab. Select images you want to process. If 'process new images' is checked in the last step, all images following the selected images will also be processed and the software will wait for new images indefinitely. If 'process new images' is left unchecked only the selected images will be processed.
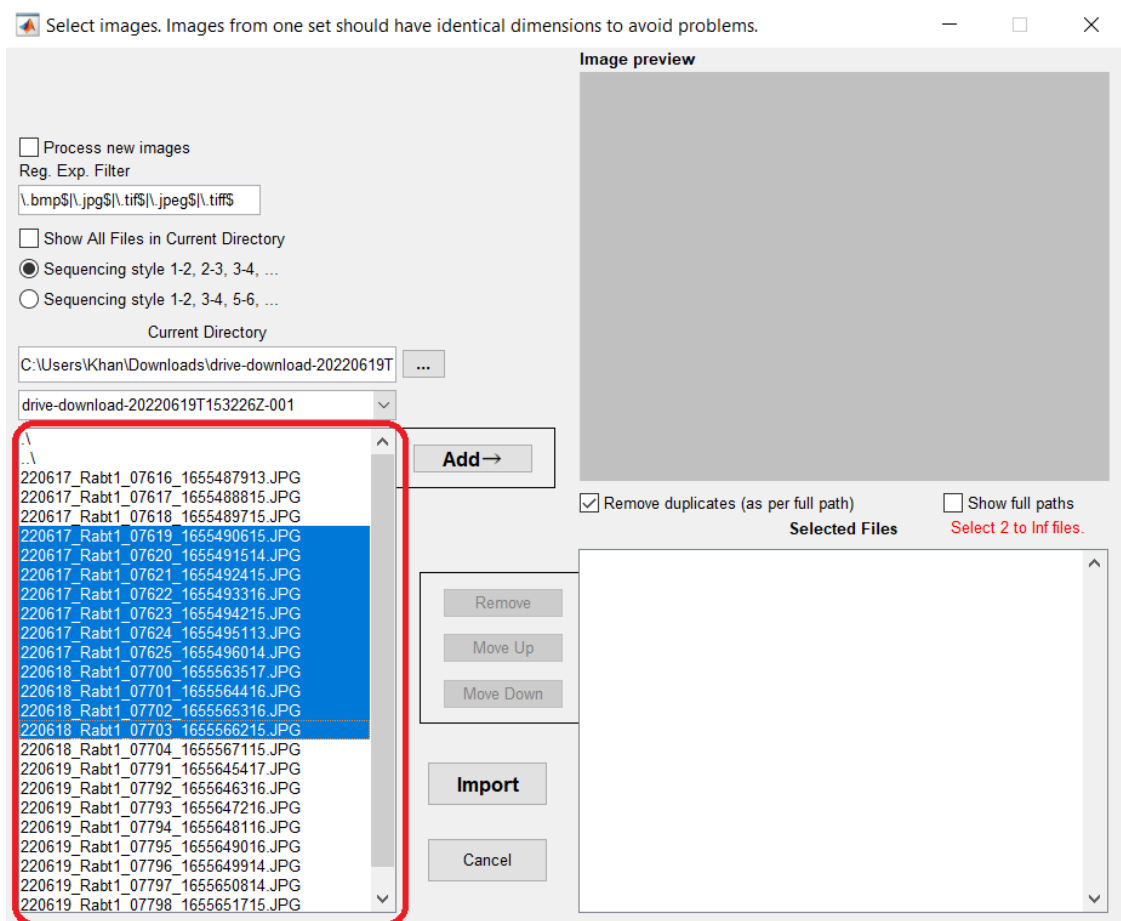
5. After selecting images click add button and the selected images will show up on the right tab. Click import to load these images to PIVlab.
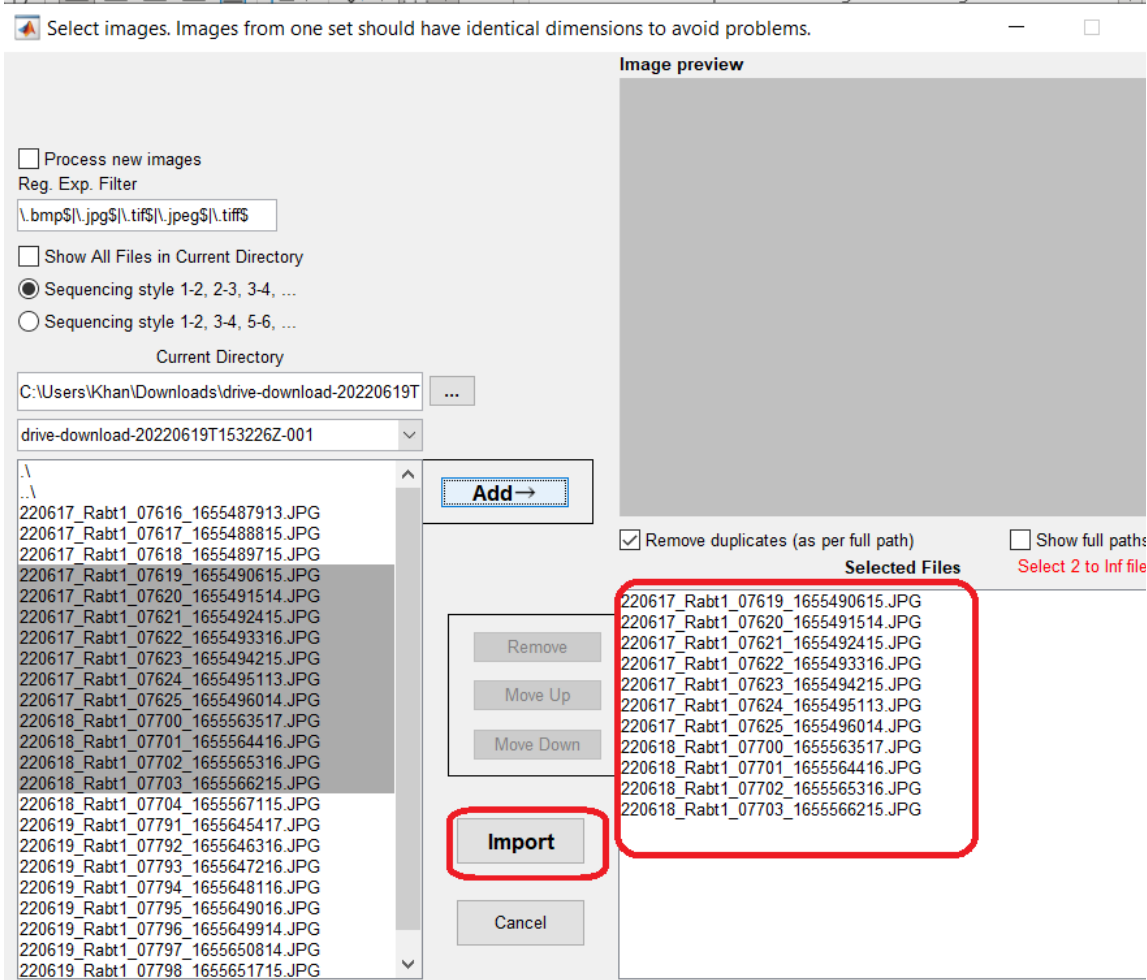
6. Click Image settings -> Exclusions
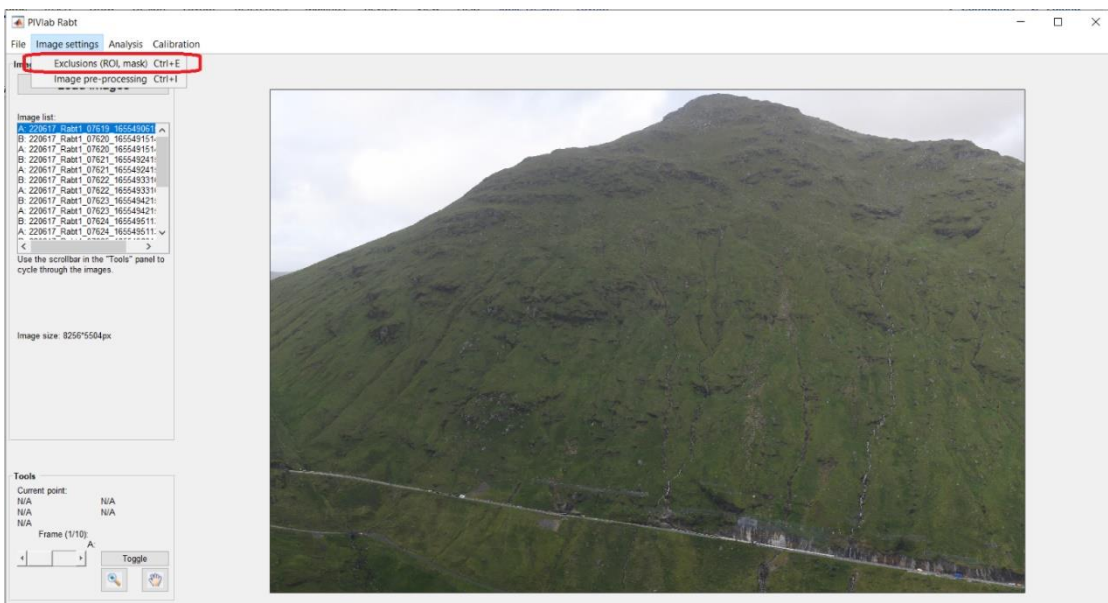
7. Buttons on this screen selects the region of interest and are defined as:

1. Select rectangular region of interest.
2. save rectangular region of interest.
3. save free hand region of interest.
4. load free hand/rectangular region of interest.
5. select free hand region of interest.
6. save free hand region of interest,

For example click 'Draw hand ROI' and then draw the region of interest on the image.
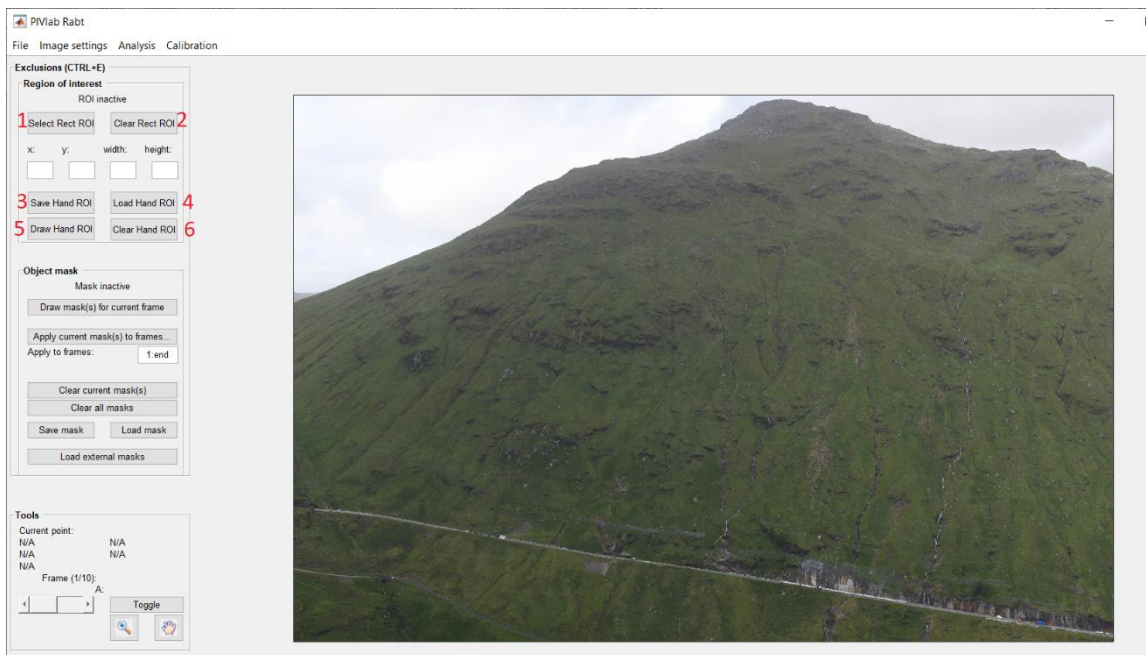
8. Click Calibration from the menu or Ctrl+z to go to calibration screen. Calibration screen has the following options:

1. PIVlab needs to know how much distance is covered by one pixel. This is called real distance. To set this up click 'Select reference distance', then click two points on the image. You need to put the distance between the two points on the image. This distance is plugged in the 'real distance' dialog box. This distance should be in mm.
2. This is the time duration between to consecutive images. We can ignore this as the time duration is calculated from the meta data of the images. To calculate the duration from meta data check the 'Real time' checkbox (6).
3. This is the filter strength. A high filter strength eliminates noise but will also remove small movements. Ideal values are between 2 to 6 but it depends upon the picture quality. A crisp, bright, registered image require a small filter strength to eliminate most of the noise.
4 and 5. These two values define the threshold of movement. Once this threshold is crossed and email will be sent to a desired email list with the image and velocity vectors. The region of interest is automatically divided into small sections. If the number of vectors pointing in the downward direction exceed 'No of vectors/block' i.e. value entered at 4, and if the average value of these vectors exceeds 'Avg of vectors/block' i.e. value entered at 5, only then an email will be sent.
6. Check to calculate time duration between images from meta data.
7. Check to enable email notification feature.
*8. enter one or multiple emails here. **NOTE:** multiple emails must be separated by a semicolon (;) and there should be no semicolon at the end of the last email entered. e.g. ABC@yahoo.com;XYZ@gmail.com;123@hotmail.com*
9. Click to enter all values.

It is a good idea to save all these settings which can be loaded again with one click if required. To save the settings click File -> save -> PIVlab settings. To Load click File ->load ->PIVlab settings.

9. Click on Analysis ->ANALYZE!

On the ANALYZE screen, click 'Analyze all frames' to start processing.
Processed images that cross the threshold are saved in a Folder 'Results'. This folder is generated when the first time the threshold is crossed. You can find this folder at the same location where the software is. NOTE: The folder is only created when any movement is observed that crosses the threshold.
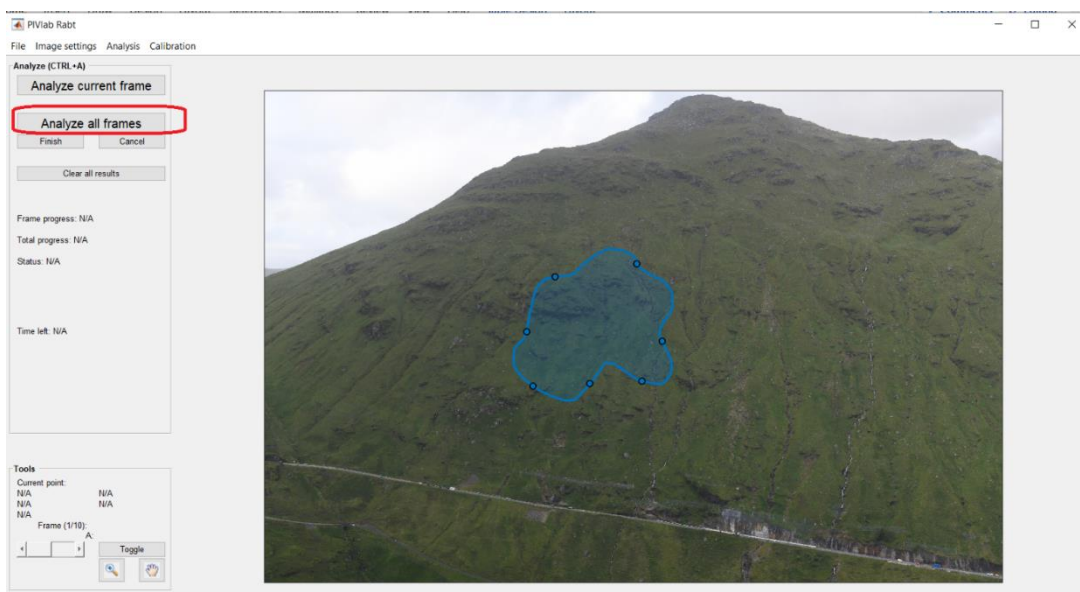
Reference

[REF1] Khan MW, Dunning S, Bainbridge R, Martin J, Diaz-Moreno A, Torun H, Jin N, Woodward J, Lim M. Low-Cost Automatic Slope Monitoring Using Vector Tracking Analyses on Live-Streamed Time-Lapse Imagery. Remote Sensing. 2021; 13(5):893. https://doi.org/10.3390/rs13050893